



## PM<sub>2.5</sub>-bound silicon-containing secondary organic aerosols (Si-SOA) in Beijing ambient air

Jingsha Xu<sup>a,b,\*</sup>, Roy M. Harrison<sup>a,c</sup>, Congbo Song<sup>a</sup>, Siqi Hou<sup>a</sup>, Lianfang Wei<sup>d</sup>, Pingqing Fu<sup>e</sup>, Hong Li<sup>f</sup>, Weijun Li<sup>g</sup>, Zongbo Shi<sup>a,\*\*</sup>

<sup>a</sup> School of Geography Earth and Environmental Science, University of Birmingham, Birmingham, B15 2TT, UK

<sup>b</sup> Department of Chemistry, University of Warwick, Coventry, CV4 7AL, UK

<sup>c</sup> Department of Environmental Sciences/Center of Excellence in Environmental Studies, King Abdulaziz University, P.O. Box 80203, Jeddah, 21589, Saudi Arabia

<sup>d</sup> State Key Laboratory of Atmospheric Boundary Layer Physics and Atmospheric Chemistry, Institute of Atmospheric Physics, Chinese Academy of Sciences, Beijing, 100029, China

<sup>e</sup> Institute of Surface-Earth System Science, Tianjin University, Tianjin, 300072, China

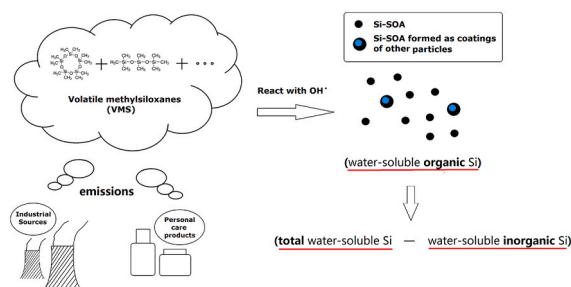
<sup>f</sup> Chinese Research Academy of Environmental Sciences, Beijing, 100012, China

<sup>g</sup> Department of Earth and Atmospheric Sciences, Zhejiang University, Hangzhou, 310027, China

### HIGHLIGHTS

- This work provided a conservative estimation of SO-Si and Si-SOA.
- Si-SOA levels were 12.7 and 36.6 ng m<sup>-3</sup> in summer and winter, respectively.
- High surface net solar radiation favors the formation of Si-SOA.
- Gas-phase oxidation is the predominant Si-SOA formation pathway.

### GRAPHICAL ABSTRACT



### ARTICLE INFO

Handling Editor: R Ebinghaus

#### Keywords:

PM<sub>2.5</sub>  
Silicon  
Secondary organic aerosol  
Volatile methylsiloxanes

### ABSTRACT

Volatile methyl siloxanes (VMS) have been widely used in personal care products and industrial applications, and are an important component of VOCs (volatile organic compounds) indoors. They have sufficiently long lifetimes to undergo long-range transport and to form secondary aerosols through atmospheric oxidation. To investigate these silicon-containing secondary organic aerosols (Si-SOA), we collected PM<sub>2.5</sub> samples during 8th-21st August 2018 (summer) and 3rd-23rd January 2019 (winter) at an urban site of Beijing. As the oxidation of VMS mainly results in hydrophilic polar semi-volatile and non-volatile oxidation products, the differences between total water-soluble Si and total water-soluble inorganic Si were used to estimate water-soluble organic Si, considered to be secondary organic Si (SO-Si). The average concentrations of SO-Si during the summer and winter campaigns were 4.6 ± 3.7 and 13.2 ± 8.6 ng m<sup>-3</sup>, accounting for approximately 80.1 ± 10.1% and 80.2 ± 8.7% of the total water-soluble Si, and 1.2 ± 1.2% and 5.0 ± 6.9% of total Si in PM<sub>2.5</sub>, respectively. The estimated Si-SOA concentrations were 12.7 ± 10.2 ng m<sup>-3</sup> and 36.6 ± 23.9 ng m<sup>-3</sup> on average in summer and winter, which accounted for 0.06 ± 0.07% and 0.16 ± 0.22% of PM<sub>2.5</sub> mass, but increased to 0.26% and 0.92% on certain days.

\* Corresponding author. School of Geography Earth and Environmental Science, University of Birmingham, Birmingham, B15 2TT, UK.

\*\* Corresponding author.

E-mail addresses: [jingsha.xu@warwick.ac.uk](mailto:jingsha.xu@warwick.ac.uk) (J. Xu), [Z.Shi@bham.ac.uk](mailto:Z.Shi@bham.ac.uk) (Z. Shi).

<https://doi.org/10.1016/j.chemosphere.2021.132377>

Received 16 June 2021; Received in revised form 15 September 2021; Accepted 25 September 2021

Available online 29 September 2021

0045-6535/© 2021 Elsevier Ltd. All rights reserved.

We found that net solar radiation is positively correlated with SO–Si levels in the summer but not in winter, suggesting seasonally different formation mechanisms.

## 1. Introduction

Silicon (Si)-containing compounds such as siloxane and polysiloxane (silicone) are widely used in personal care products and industrial applications. They have a high potential to form secondary organic aerosols (SOA). Recent studies of Si-containing SOA (Si-SOA) from oxidation of siloxanes include: physical properties characterization of Si-SOA produced from an oxidation flow reactor (OFR) (Janeček et al., 2019), molecular characterization of Si-SOA with high-performance mass spectrometry (Wu and Johnston, 2016, 2017), experimental and theoretical investigation of the kinetics and mechanism of volatile methylsiloxanes (VMS) oxidation by hydroxyl radical (Xiao et al., 2015), modelling for the estimation of the production rates of dimethylsilanediol (DMSD) from VMS (Muirhead et al., 2018), modelling for quantification of three VMS and their oxidation products (Janeček et al., 2017), and assessment of health impacts of Si-SOA on human lung cells (King et al., 2020). Due to the complex oxidation processes of siloxanes to form various types of Si-SOA (Xiao et al., 2015), the total concentration of Si-SOA has never been reported.

The main sources of silicon in the troposphere include resuspended silicon containing dust from natural or anthropogenic sources and emissions of silicon-containing compounds, such as from industry and fuel consumption (Wang et al., 2001). Organosilicon compounds have not been identified in natural sources (Muirhead et al., 2018), and therefore, organosilicon compounds are assumed to arise mainly from human activities. It was reported that siloxanes were the most abundant volatile organic compounds (VOCs) emitted from a university classroom (Tang et al., 2015).

All siloxanes with the number of silicon atoms  $>1$  are considered to be oligomers or polymers. The global production of polysiloxane is enormous. China was the largest manufacturer and consumer of polysiloxane in the world in 2009, with the output and consumption of 270 000 and 430 000 tons in 2009, respectively (CRCSI, 2010). In 2018, the output and consumption of polysiloxane in China has reached 1.04 and 1.13 million tons, respectively (CBIRI, 2019). Organosilicon compounds like methyl siloxanes are widely applied in industrial applications and consumer products due to their high thermal stability, water repellence, smooth texture and low surface tension (Xu et al., 2015). VMS, polydimethylsiloxane and polyethermethylsiloxane are three organosilicon classes, which have noteworthy environmental loadings (Wang et al., 2013). The hydrolysis or thermal decomposition of polydimethylsiloxane and polyethermethylsiloxane can also generate highly volatile cyclic dimethylsiloxanes or volatile linear siloxane diols such as dimethylsilanediol (Tuazon et al., 2000; Wang et al., 2001).

VMS can be classified as volatile linear or cyclic methylsiloxanes. Consisting of  $-(\text{CH}_3)_2\text{SiO}-$  structural units, linear- (IVMS) and cyclic-volatile methylsiloxanes (cVMS) are widely used in cleaning agents, lubricants, and personal care products, such as cosmetics, antiperspirants, and skin and hair care products (Horii and Kannan, 2008; Wang et al., 2009a; Xiao et al., 2015). Worldwide production of cVMS is huge, with cVMS production in the European Union and North America nearly 100 million kg per year (Xiao et al., 2015), and more than 90% of the environmental loading of cVMS in the United States in 1993 was released to the atmosphere, with the remaining cVMS discharged to wastewater (Genualdi et al., 2011). China is leading the world in the production capacity of cyclic siloxanes, with its production reaching about 800 million kg in 2008 (Xu et al., 2013). cVMS can easily partition into the atmosphere as vapour due to their low water solubilities, high Henry's Law constants and high vapour pressures (Wang et al., 2013). The environmental properties and consequent concerns over cVMS, such as bioaccumulation, toxicity, and degradation, were addressed in a

review paper on organosiloxanes (Rücker and Kümmerer, 2015). A number of cVMS including octamethylcyclotetrasiloxane (D4), decamethylcyclopentasiloxane (D5), and dodecamethylcyclohexasiloxane (D6) have been prioritized in several regulatory jurisdictions due to their persistence and bioaccumulation potential and environmental toxicity (Kierkegaard and McLachlan, 2013; Wang et al., 2013). In indoor air samples collected from the UK and Italy, the average concentration of IVMS (L2~L5) and cVMS (D3~D6) together could reach  $240 \mu\text{g m}^{-3}$  in Italy and  $350 \mu\text{g m}^{-3}$  in the UK (Pieri et al., 2013). The half-lives of L3 and L4 are reported as 8.77 and 6.03 days, respectively (Whelan et al., 2004), while for D3, D4 and D5, they can extend to around 10–30 days (Xiao et al., 2015), which indicates that they can exist in the atmosphere sufficiently long to undergo oxidation to generate secondary products and long-range transport to affect air quality regionally. The atmospheric half-lives and concentrations of some major IVMS and cVMS in the outdoor environment are summarized in Table 1.

Because of the increasing production and consumption of VMS, many studies have been conducted to investigate their physical/chemical properties (Xu and Wania, 2013; Xu et al., 2014), develop analytical methods (Badjagbo et al., 2009; Kierkegaard et al., 2010), and to determine their atmospheric concentrations (Genualdi et al., 2011; Kierkegaard and McLachlan, 2013; Lu et al., 2010; Krogseth et al., 2013; Buser et al., 2013) as well as their bioaccumulation effects (Kierkegaard et al., 2011, 2013). Si has been detected in atmospheric nanoparticles, which occurred in up to 50% of atmospheric nanoparticles with a mole fraction  $>0.01$  in Pasadena, suggesting the possible contribution from Si-containing VOCs to nanoparticulate Si formation through photochemical reactions (Bzdek et al., 2014).

VMS compounds may undergo oxidation with atmospheric oxidants to form new particles or partition onto existing particles. VMS were reported not to be reactive toward ozone and  $\text{NO}_3$  radicals (Kim and Xu, 2017). The predominant degradation pathways of atmospheric VMS is through oxidation of vapour by hydroxyl radical, which can produce compounds including silanols, silanediols and silanetriols (Wu and Johnston, 2017; Xiao et al., 2015). A previous study showed that the reaction with hydroxyl radical in the first oxidation step is a major VMS degradation pathway (Kim and Xu, 2017). The hydroxyl radical is reported to be abundant (Slater et al., 2020) and to play an important role in the atmospheric chemistry of Beijing (Whalley et al., 2021). It is reported that the silanols can quickly partition into the particle phase in the atmosphere (Chandramouli and Kamens, 2001). Chamber studies have shown that the nonvolatile and semi-volatile oxidation products of VMS by OH radical can form secondary aerosols (Chandramouli and Kamens, 2001; Wu and Johnston, 2016, 2017). Wu and Johnston (2016) investigated the chemical composition of secondary aerosol formed from D4 and D5 oxidation by OH radical, which showed that the oxidation led predominantly to the substitution of one or more  $\text{CH}_3$  groups by OH,  $\text{CH}_2\text{OH}$  or  $\text{CH}_2\text{OOH}$  groups. Due to the various pathways of the VMS oxidation process and numerous oxidation products (Lamaa et al., 2014; Wu and Johnston, 2017; Xiao et al., 2015), it is difficult to identify all oxidation products, and to quantify all of them in ambient aerosol samples. In the work of Janeček et al. (2017), they calculated the concentrations of the oxidation products of D5 (namely o-D5) applying a Community Multiscale Air Quality (CMAQ) model with the experimentally determined D5 as input. Si-SOA tracers in fine particles are also starting to be determined through laboratory analysis, but total Si-SOA remained unquantified (Milani et al., 2021).

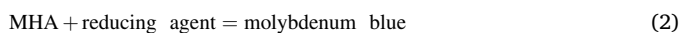
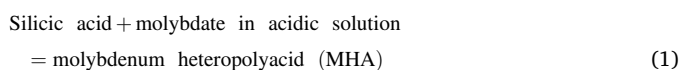
In this work, we propose a conservative estimation of SO–Si and Si-SOA, which does not require information on the precursor concentrations to estimate the SO–Si and Si-SOA concentrations in ambient fine particles for the first time.

## 2. Experimental

### 2.1. Method introduction

The introduction of hydroxyl groups into IVMS and cVMS molecules improves their attractive interactions with water molecules, which leads to an increase of the water solubility the VMS oxidation products (Wang et al., 2013; Atkinson, 1991; R ucker and K ummerer, 2015). Compounds like dimethylsilanediol (DMSD) and methylsilanetriol (MST) are extremely water soluble (Muirhead et al., 2018; R ucker and K ummerer, 2015). The water solubility of (CH<sub>3</sub>)<sub>3</sub>SiOH is 7.2 g/100 g H<sub>2</sub>O and 1, 2-dihydroxytetramethyldisilane is 12.4 g/100 g H<sub>2</sub>O (R ucker and K ummerer, 2015). Because the absolute mass of PM<sub>2.5</sub> on the filters for extraction are usually very low (<4 mg per 10 mL water in this study) and the absolute mass of Si-SOA are even lower, all Si-SOA should be solubilized in water extracts considering the relatively high solubility (grams per 100 mL water) of Si-SOA. On the other hand, primary organosilicon compounds are hydrophobic, and polydimethylsiloxanes are almost insoluble in water (R ucker and K ummerer, 2015). Therefore, the water-soluble Si-containing organic compounds are considered to be secondary reaction products. By subtracting water-soluble inorganic Si from total water-soluble Si, the remainder is water-soluble organic Si, and can be treated as SO-Si. This can provide a conservative estimate of Si-SOA concentrations in fine particles. Advantages of this method include the practicable quantification of Si-SOA without the necessity to identify and quantify all oxidation products of VMS, ease and speed of analysis, no involvement of organic solvents, and no need of knowing the concentrations of VMS.

The total water-soluble Si can be analysed by Inductively Coupled Plasma- Optical Emission Spectrometer (ICP-OES). Inorganic Si-containing compounds like silica (SiO<sub>2</sub>) or its polymeric solid form-(SiO<sub>2</sub>)<sub>x</sub> are almost insoluble in water. Soluble inorganic Si compounds or molybdate-reactive silica include dissolved simple silicates, monomeric silica and silicic acid, and an undetermined fraction of polymeric silica. The pH of the solution and the type and composition of the silicon-containing aerosols are the primary factors controlling both the form and solubility of silica in the resulting solution. It can exist as silicic acid or silicate ion in solution depending upon pH. For example, silica presents predominantly as silicic acid at pH < 9 (Martin, 2007), and almost completely as silicic acid at pH < 7, while silicate ions become increasingly more abundant when pH is increased to around 10 (Annenkov et al., 2017). Hence, in acidic solution (pH < 7), they can be determined by the traditional colorimetric method based on molybdenum blue, shown as Eqs. (1) and (2) (Giacomelli et al., 1999; ASTM, 1990):



In Eq. (2), the reducing agent could be 1-amino-2-naphthol-4-

sulphonic acid (ANS, applied in this study) or ascorbic acid or *p*-methylanilino-phenol sulfate. Turbidity and colour will interfere in the colorimetric analysis, and they should be removed by filtration and dilution. Phosphate is the only specific compound known to interfere in the colour reaction, and its interference is eliminated by adding oxalic acid (Giacomelli et al., 1999).

### 2.2. Sampling

In this work, summer and winter PM<sub>2.5</sub> samples collected in Beijing were chosen and compared for better understanding of Si-SOA formation under different atmospheric conditions. PM<sub>2.5</sub> samples were collected on 47 mm PTFE filters at an urban site located at the Institute of Atmospheric Physics (IAP: 116.39°E, 39.98°N) of the Chinese Academy of Sciences in Beijing, China during summer (8th-21st August 2018) and winter (3rd-23rd January 2019) for 23 h each day by medium volume samplers (Zambelli, Italy) at a flow rate of 38.3 L min<sup>-1</sup>. The 47 mm PTFE filters were chosen because the Si background from the filter-making materials is extremely low and they have low water uptake and can be used for weighing. Other commonly used filter materials, such as quartz or cellulose filters cannot be used either because they are composed of silicon dioxide or are not suitable for weighing. Due to a sampler connection problem, the sampling on 4th January was not successful, and hence, this day was excluded for analysis. Field blanks were collected every five days. All chemical concentrations were corrected by the values obtained from field blanks. Hourly PM<sub>2.5</sub> mass concentrations were obtained via the China National Environmental Monitoring Network (CNEM) website from a nearby Olympic Park station which is around 1 km away from the sampling site of IAP, and the original hourly data was averaged to 24 h for daily comparison. Our previous study has showed that the PM<sub>2.5</sub> data at this station are close to those observed at IAP (Shi et al., 2019). The closeness of observed PM<sub>2.5</sub> concentrations at different air quality stations in Beijing also provides further reassurance of the representative nature of the observed PM<sub>2.5</sub> concentration at the Olympic Park station (Shi et al., 2019; Xu et al., 2020b).

### 2.3. Meteorological data

Hourly meteorological data, including wind speed (ws), air temperature (temp), and relative humidity (RH), were obtained from the NOAA National Center for Environmental Information for the Beijing-Capital international airport station, which is around 20 km away from the sampling site of IAP (available at: <https://gis.ncdc.noaa.gov/maps/ncei/cdo/hourly>; last access: May 2020). ERA5 hourly data of surface net solar radiation (ssr), downward UV radiation at the surface (uvb) (this parameter is the amount of ultraviolet (UV) radiation reaching the surface.), total cloud cover (tcc), and total precipitation (tp) were acquired from the Copernicus Climate Change Service (C3S), available at: <https://cds.climate.copernicus.eu/cdsapp#!/dataset/reanalysis-era5-single-levels?tab=form> (last access: May 2020). All hourly

**Table 1**  
Atmospheric outdoor concentrations of major IVMS and cVMS compounds (ng m<sup>-3</sup>).

		L3	L4	L5	L6	D3	D4	D5	D6	References
Toronto, Canada (Semiurban)	2010–2011	1.3 ± 1.0	2.1 ± 1.3	1.9 ± 1.0		1.6 ± 1.1	16 ± 12	91 ± 54	7.3 ± 4.2	Ahrens et al. (2014)
Guangzhou, China (Urban)	1996					2900	900			Wang et al. (2001)
Paris, France (Urban)	2009	0.029	0.057	0.12		30	50	280	53	Genualdi et al. (2011)
Downsview, ON, Canada (Urban)	2009	0.12	0.66	0.45		18	11	55	6.2	
Sydney, FL, USA (Urban)	2009		0.16	0.081		0.65	5.4	82	4.0	
Chicago, USA (Urban)							18–190	100–1100	0–50	Yucuis et al. (2013)
Tystberga, Sweden (regional background)	2011	0.2	0.025	0.013	0.022	0.94	3.5	13	1.0	Kierkegaard and McLachlan (2013)

Note: L3: Octamethyltrisiloxane; L4: Decamethyltetrasiloxane; L5: Dodecamethylpentasiloxane; L6: Tetradecamethylhexasiloxane; D3: Hexamethylcyclotrisiloxane; D4: Octamethylcyclotetrasiloxane; D5: Decamethylcyclopentasiloxane; D6: Dodecamethylcyclohexasiloxane.

data were averaged as daily data, corresponding to the sampling times.

#### 2.4. Reagents and solutions preparation

All solutions were prepared with reagent grade chemicals and stored in clean polyethylene or plastic bottles at 4 °C. Milli Q water (Millipore Corp.) was used for the preparation of all solutions and dilutions. All chemical solutions were filtered through 0.22 µm filters before use.

##### (1) Silicon standard solution

The  $1000 \pm 2 \text{ mg Si L}^{-1}$  silicon standard for ICP in 2% NaOH (Sigma-Aldrich) and the silicon standard solution containing  $1000 \pm 4 \text{ mg Si L}^{-1}$  in 2% NaOH (Silicon standard for AAS, Sigma-Aldrich) were cross-calibrated by using both UV/Vis and ICP-OES, giving identical results. Hence, in order to eliminate the impact of using two different Si standards, the  $1000 \pm 4 \text{ mg Si L}^{-1}$  silicon standard in 2% NaOH (Silicon standard for AAS, Sigma-Aldrich) was selected to prepare the standard solutions for external calibrations of both UV/Vis and ICP-OES.

##### (2) Ammonium molybdate solution

Ammonium molybdate solution ( $75 \text{ g L}^{-1}$ ) was prepared by dissolving 7.5 g of ammonium molybdate tetrahydrate ( $(\text{NH}_4)_6\text{Mo}_7\text{-O}_{24}\cdot 4\text{H}_2\text{O}$ ) in 50 mL of water, adding 8.5 mL of  $\text{H}_2\text{SO}_4$  (96%) and adding water to a total volume of 100 mL.

##### (3) Amino-2-naphthol-4-sulfonic acid (ANS) solution

The reducing solution was prepared by dissolving 0.5 g of 1-amino-2-naphthol-4-sulfonic acid (ANS) in 50 mL of a solution containing 1 g of sodium sulfite ( $\text{Na}_2\text{SO}_3$ ). After dissolving, the solution was added to a 100 mL solution containing 30 g of sodium hydrogen sulfite ( $\text{NaHSO}_3$ ). The mixture was made up to 200 mL with ultrapure water and stored in a dark, plastic bottle.

##### (4) Oxalic acid

Oxalic acid ( $\text{H}_2\text{C}_2\text{O}_4\cdot 2\text{H}_2\text{O}$ ) is used to minimize the phosphate response, whilst having little effect on the silicate response (Giacomelli et al., 1999).  $100 \text{ g L}^{-1}$  oxalic acid solution was prepared by dissolving 10 g of oxalic acid ( $\text{H}_2\text{C}_2\text{O}_4\cdot 2\text{H}_2\text{O}$ ) in 100 mL of water (ASTM-International, 2016).

#### 2.5. Sample extraction

One half of the 47 mm PTFE filter (including samples and field blanks) was extracted ultrasonically with 10 mL water for 30 min at room temperature and stood for another 30 min before filtered with 0.22 µm filters. Blank filters of the same size were spiked with 20 µL of  $100 \text{ mg L}^{-1}$  standard solution. After dryness, the spiked filters were extracted with 10 mL water applying the same extraction method for a recovery test. The sample extracts were analysed within 2 days by both ICP-OES and UV/Vis.

#### 2.6. UV/Vis analysis

5 mL of the extracts was transferred into 15 mL polyethylene metal free centrifuge tubes and diluted to 10 mL. The interference of the colour of the extracts was removed by further dilution until the extracts were nearly colorless and transparent using white paper as the background. After this step, 0.4 mL of the ammonium molybdate solution was added and mixed well with the diluted extracts. After 5 min, 0.3 mL of the oxalic acid solution was added and mixed well with the solutions. After 1 min, 0.4 mL of the ANS solution was added and mixed well, and further stood for 10 min. Reagent blank and standards were prepared by

treating 10 mL aliquots of Milli Q water and silicon standards of different levels ( $1\text{--}200 \text{ µg Si L}^{-1}$ ) in the same procedure as mentioned above. The absorbance of the samples and standards was measured at 815 nm against the reagent blank by a spectrophotometer (JENWAY 6800 UV/Vis). Longer path length cells (4 cm) which were recommended for concentrations below  $100 \text{ µg L}^{-1}$  were used for the test (ASTM-International, 2016). A good calibration curve was obtained between 1 and  $200 \text{ µg Si L}^{-1}$  with  $R^2 = 0.9999$  between absorbance and concentration (Fig. S1). The recoveries of spiked filter blanks were 100.0%~109.9% (mean: 104.5%) (Table S1). Blanks, standards and duplicates were run every 10 samples. Each sample was tested 3 times and their average was used for the calculation of the concentration. The calculated detection uncertainty (standard deviation of standards run every 10 samples) was less than  $0.1 \text{ µg Si L}^{-1}$ . Two sets of standards were made before the sample extraction and before UV/Vis detection, and the differences of the concentrations calculated using the two calibration curves were  $<0.39 \text{ µg Si L}^{-1}$ . The detection limit (DL), calculated as 3 times the standard deviation (SD) of blanks was  $1.4 \text{ µg Si L}^{-1}$ , corresponding to approximately  $0.6 \text{ ng m}^{-3}$ . Each sample and standard were measured three times, the relative standard deviation (RSD) ranged between 0.1–7.8% (mean: 2.0%) for samples and 0.0–3.1% (mean: 1.2%) for standards. Two identical filter cuts from each sample ( $n = 8$ ) were extracted separately in the same manner to test the repeatability, which ranged between 0.1–16.2% (mean: 8.8%). Standard tests were also run for the water-soluble organic Si compound-Heptamethylcyclotetrasiloxan-2-ol ( $\text{D3D}^{\text{OH}}$ ), and the results showed  $< \text{DL}$  on UV/Vis for inorganic Si concentrations (Table S2).

#### 2.7. ICP-OES analysis

Inductively Coupled Plasma- Optical Emission Spectrometry (ICP-OES, Optima 8000) was applied to determine the total water-soluble Si concentrations. The extraction recovery ranged between 110.3% and 116.2% (mean: 113.1%). A good calibration curve was obtained between 10 and  $200 \text{ µg Si L}^{-1}$  with  $R^2 = 0.9999$  (Fig. S2). The detection limit, calculated as 3 times the standard deviation (SD) of blanks, was  $4.8 \text{ µg L}^{-1}$ , equivalent to  $2.0 \text{ ng m}^{-3}$  in the air. Each sample and standard were measured three times, and the relative standard deviation (RSD) ranged between 0.2 and 8.8% (mean: 2.0%) for samples and 0.6–8.7% (mean: 3.0%) for standards. Two identical filter cuts from each sample ( $n = 8$ ) were extracted separately in the same manner to test the repeatability, which ranged between 4.8 and 16.9% (mean: 10.5%). The uncertainty budget for the estimation of total water-soluble Si, total water-soluble inorganic Si and SO-Si is provided in the supplemental information. The combined standard uncertainty of SO-Si as a percentage ( $u_{\text{or}}$ ) is 27.2%, which is calculated using the combined standard uncertainty of total water-soluble Si ( $u_{\text{t}}$ ) and total water-soluble inorganic Si ( $u_{\text{in}}$ ).

#### 2.8. Backward trajectory and cluster analysis

The air mass backward trajectories were obtained from the Hybrid Single-Particle Lagrangian Integrated Trajectory (HYSPPLIT) model, which was developed by the NOAA Air Resources Lab (Stein et al., 2015; Rolph et al., 2017). Each trajectory was computed from archived global data assimilation system (GDAS1, 2006-present) meteorological data with a duration of 72h. The trajectories started at 8:00 a.m. local time with 6-h intervals on each sampling day at 500 m above ground level (AGL). Then these computed trajectories were clustered in a geographic information system (GIS) based software, namely TrajStat 1.2.1.0 (Wang et al., 2009b). The Euclidean distance-based calculation was applied to merge those trajectories with similar origins.

### 3. Results and discussion

#### 3.1. Atmospheric lifetimes and backward trajectory analysis

The approximate lifetimes of VMS compounds and their oxidation products were calculated based on the average OH radical concentrations measured in Beijing. As the OH concentrations varies significantly ( $<1 \times 10^6$ – $1.7 \times 10^7$  molecules  $\text{cm}^{-3}$ ) during different hours of the day, and also varies in different seasons and under different weather conditions (Lu et al., 2013; Chu et al., 2021), the OH concentrations used for the calculation of atmospheric lifetimes are daily averaged concentrations during each season. The average OH concentrations for the calculation of VMS lifetimes in this study were assumed to be  $4.9 \times 10^6$  mol  $\text{cm}^{-3}$  in summer (Rao et al., 2016), and  $1.5 \times 10^6$  mol  $\text{cm}^{-3}$  in winter (Chu et al., 2021). However, it should be noted that the OH concentration applied for summer ( $4.9 \times 10^6$  mol  $\text{cm}^{-3}$ ) was not a daily average, but a modeled daytime average in a non-haze period. Apart from OH concentration as an important factor affecting VMS atmospheric lifetimes, the sensitivity of their atmospheric lifetimes to other factors such as variation in the time-of-day for VMS emissions, and to relative humidity dependent heterogeneous uptake and/or reactions on mineral dusts are assessed in Navea et al. (2011). They found that VMS lifetime was insensitive to urban OH concentrations due to limited residence time, and somewhat sensitive to enhanced OH levels in the transition area between the urban and rural locations.

As shown in Table 2, the lifetimes of these compounds ranged from

**Table 2**  
Calculated lifetimes of VMS compounds and oxidation products in Beijing.

Molecule	$K_{\text{OH}} (\times 10^{-12} \text{ cm}^3 \text{ mol}^{-1} \text{ s}^{-1})$	Approximate lifetime (t; days)		References
		Summer	Winter	
L1	$1.0 \pm 0.27$	2.36	7.72	Atkinson (1991)
	$1.28 \pm 0.46$	1.85	6.03	Sommerlade et al. (1993)
L2	$1.38 \pm 0.36$	1.71	5.59	Atkinson (1991)
	$1.19 \pm 0.30$	1.98	6.48	Sommerlade et al. (1993)
	$1.32 \pm 0.05$	1.79	5.85	Markgraf and Wells (1997)
	$1.20 \pm 0.09$	1.97	6.43	Alton and Browne (2020)
L3	$1.83 \pm 0.09$	1.29	4.22	Markgraf and Wells (1997)
	$1.7 \pm 0.1$	1.39	4.54	Alton and Browne (2020)
L4	$2.66 \pm 0.13$	0.89	2.90	Markgraf and Wells (1997)
	$2.5 \pm 0.2$	0.94	3.09	Alton and Browne (2020)
L5	$3.4 \pm 0.5$	0.69	2.27	Alton and Browne (2020)
D3	$0.86 \pm 0.09$	2.75	8.97	Alton and Browne (2020)
D4	$1.01 \pm 0.32$	2.34	7.64	Atkinson (1991)
	$1.26 \pm 0.40$	1.87	6.12	Sommerlade et al. (1993)
	$1.3 \pm 0.1$	1.82	5.94	Alton and Browne (2020)
D5	$1.55 \pm 0.49$	1.52	4.98	Atkinson (1991)
	$2.1 \pm 0.1$	1.12	3.67	Alton and Browne (2020)
MDOH	$1.89 \pm 0.60$	1.25	4.08	Whelan et al. (2004)
MOH	$3.95 \pm 0.95$	0.60	1.95	Sommerlade et al. (1993)

Note: L1: Tetramethylsilane; L2: Hexamethyldisiloxane; MDOH: Pentamethyldisiloxanol; MOH: Trimethylsilanol.  $K_{\text{OH}}$  is the rate constant for oxidation by OH radicals; The approximate lifetimes of these compounds were calculated as:  $t = [1/(K_{\text{OH}} \times C_{\text{OH}})] / (60 \times 60 \times 24)$ ;  $C_{\text{OH}}$  is the average concentration of OH radicals in Beijing, which is  $4.9 \times 10^6$  (Rao et al., 2016), and  $1.5 \times 10^6$  (Chu et al., 2021) mol  $\text{cm}^{-3}$  in summer and winter, respectively.

1.95–7.72 and 0.60–2.75 days in summer and winter, respectively. For the most abundant species D4 and D5, their lifetimes range from 1.12–2.34 and 3.67–7.64 days in summer and winter, respectively.

The cluster results of the 72-hr backward trajectories are shown in Fig. 1. In summer, the cluster results of the backward trajectory analysis show that around half of the trajectories (30% + 18%) were ocean originated, while 32% (9% + 23%) and 20% of the trajectories were from Mongolia and Helongjiang Province, respectively. The trajectories in summer did not pass heavily polluted cities such as Ulaanbaatar or Baotou (Hasenkopf et al., 2016; Zhou et al., 2016). However, all of the backward trajectories in winter had terrestrial origins, and 26% of the trajectories were from inner Mongolia and passed Baotou before arriving Beijing. The remaining trajectories (74%) were from Russia and passed Mongolia, and 27% of them passed Ulaanbaatar. In addition, all trajectories also passed heavily polluted northern Hebei province in winter, while only half of them passed this region in summer. Hence, apart from local sources, the aerosol levels in winter of Beijing may be more influenced by long-range transport, especially from heavily polluted regions.

#### 3.2. $p.m_{2.5}$ and total Si concentrations

In summer (August 2018), daily  $\text{PM}_{2.5}$  concentrations ranged from 10.9 to 55.3  $\mu\text{g m}^{-3}$  (mean:  $29.4 \pm 15.9 \mu\text{g m}^{-3}$ ). While in winter (January 2019), daily  $\text{PM}_{2.5}$  concentrations ranged from 8.4 to 260.8  $\mu\text{g m}^{-3}$ , with an average of  $57.5 \pm 56.2 \mu\text{g m}^{-3}$ , approximately double that in the summer period. The highest daily concentration of  $\text{PM}_{2.5}$  in winter was 260.8  $\mu\text{g m}^{-3}$ , much higher than the China National Ambient Air Quality Standard (CNAAQS) (BG3095-12) Grade II for 24 h average  $\text{PM}_{2.5}$  concentration (75  $\mu\text{g m}^{-3}$ ). Elevated  $\text{PM}_{2.5}$  levels in winter could be attributed to regional transport, stagnant weather and increased local emissions due to house heating etc.

As total Si was not determined in this study, it is estimated by applying a total-Si/ $\text{PM}_{2.5}$  ratio. In our previous study (Xu et al., 2020a),  $\text{PM}_{2.5}$  samples were collected in the same sampling location and the mean total-Si/ $\text{PM}_{2.5}$  ratios in winter 2016 and summer 2017 were 1.14% and 1.95%, respectively. Both ratios (overall mean: 1.55%) are comparable to the annual mean Si abundance in  $\text{PM}_{2.5}$  samples (1.56%) collected in Beijing in 2013 (Lu et al., 2019). Hence, the total-Si/ $\text{PM}_{2.5}$  ratios of 1.14% and 1.95% were applied to estimate the total Si concentrations in winter and summer in this study, respectively.

The estimated total-Si concentrations ranged between 0.21 and 1.08 and 0.10–2.97  $\mu\text{g m}^{-3}$  in summer and winter, respectively. The average concentrations of total-Si in summer and winter were  $0.57 \pm 0.31$  and  $0.66 \pm 0.64 \mu\text{g m}^{-3}$ , respectively. These results are lower than those reported in Beijing during 2000, which showed the total-Si in  $\text{PM}_{2.5}$  during July and January were 1.87 and 0.99  $\mu\text{g m}^{-3}$ , respectively, accounting for 1.9% and 1.6% of  $\text{PM}_{2.5}$  (Song et al., 2006). These are also lower than those from another study carried out at an urban site of Beijing, in which the total Si concentration was  $1.0 \pm 0.9 \mu\text{g m}^{-3}$ , accounting for 1.2% of  $\text{PM}_{2.5}$  (Li et al., 2017b). This is consistent with the reduction in  $\text{PM}_{2.5}$  levels (Vu et al., 2019) and in the emissions of crustal compounds.

#### 3.3. Total water-soluble Si, water-soluble inorganic and organic Si

Fig. 2 shows total water-soluble Si (i.e., water-soluble inorganic and organic Si) determined through the ICP-OES analysis of water-extracted aerosol samples. The water-soluble inorganic Si measured by UV-Vis ranged from <DL to 3.5  $\text{ng m}^{-3}$ , with an average of  $1.0 \pm 0.8 \text{ ng m}^{-3}$  in summer. In winter, water-soluble inorganic Si was in the range of 1.0–16.1  $\text{ng m}^{-3}$ , with an average of  $3.6 \pm 3.9 \text{ ng m}^{-3}$ . The mean total water-soluble Si in winter was  $16.8 \pm 12.2 \text{ ng m}^{-3}$ , approximately 3 times higher than that of summer ( $5.6 \pm 4.0 \text{ ng m}^{-3}$ ). As mentioned in the method introduction, the difference between total water-soluble Si and water-soluble inorganic Si is water-soluble organic Si (SO-Si). The

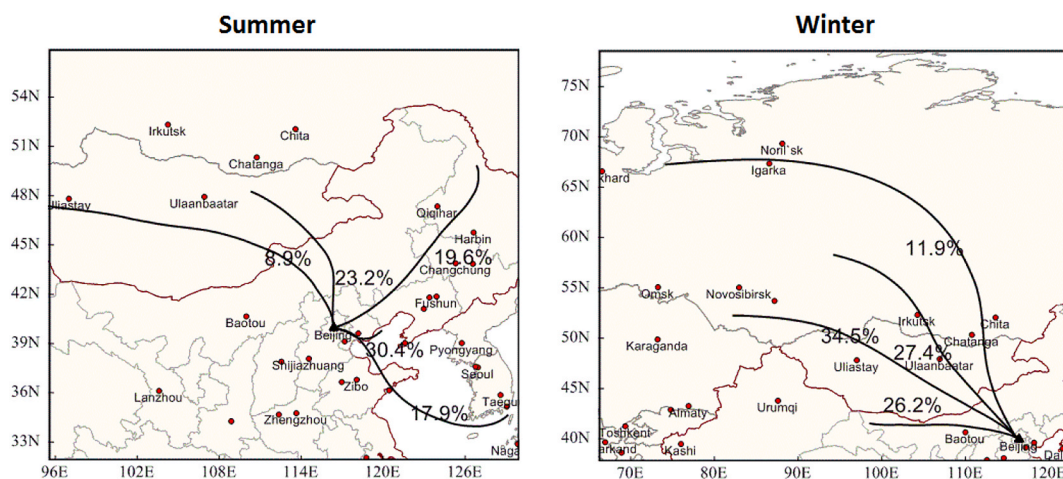


Fig. 1. Air mass backward trajectory clusters arriving at IAP during summer and winter in Beijing.

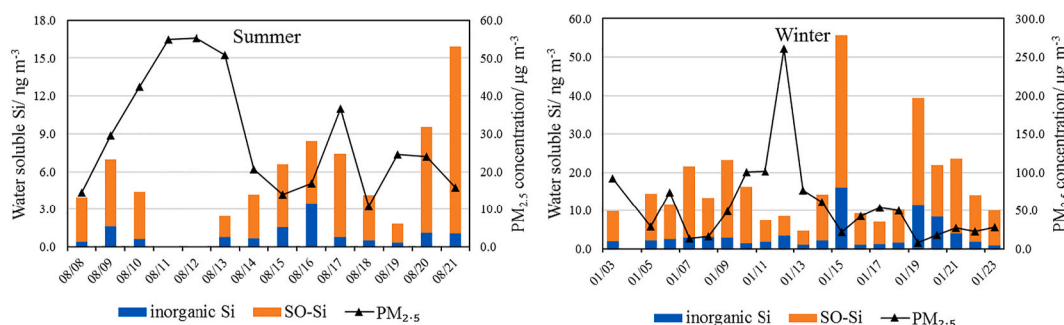


Fig. 2. Daily PM<sub>2.5</sub> concentrations, water-soluble inorganic Si (Si-inorganic) and secondary organic Si (SO-Si) concentrations at IAP, Beijing during (a) summer (August 2018) and (b) winter (January 2019) (Concentrations on 11th and 12th August are < DL).

SO-Si concentrations ranged from <DL to 14.9 ng m<sup>-3</sup> (mean: 4.6 ± 3.7 ng m<sup>-3</sup>) and 3.5–39.6 ng m<sup>-3</sup> (mean: 13.2 ± 8.6 ng m<sup>-3</sup>) in summer and winter, respectively. They account for approximately 80.1 ± 10.1% and 80.2 ± 8.7% of the total water-soluble Si, 1.2 ± 1.2% and 5.0 ± 6.9% of the total Si, and 0.023 ± 0.024% and 0.057 ± 0.079% of PM<sub>2.5</sub> mass.

Si accounts for around 38% of cVMS and 36% of lVMS according to their molecular weights (Table 3). Assuming the oxidation of VMS by OH radical would replace one H-atom in one CH<sub>3</sub> group with only one OH group, as D5 is the most abundant pollutant among these VMS (Ahrens et al., 2014; Genualdi et al., 2011; Kierkegaard and McLachlan, 2013), the Si-SOA concentration is conservatively estimated as the Si concentration dividing by the mass ratio of Si to D5-OH (one H-atom in one CH<sub>3</sub> group in D5 was replaced by one OH group) (36.2%) (Table 3). The estimated Si-SOA concentrations in summer and winter were 12.7 ± 10.2 ng m<sup>-3</sup> and 36.6 ± 23.9 ng m<sup>-3</sup>, respectively, accounting for 0.06 ± 0.07% (range <0.003–0.26%), and 0.16 ± 0.22% (0.006–0.92%) of PM<sub>2.5</sub>. Even though summer is expected to have VMS emissions due to

evaporation under higher temperature, the synoptic scale stagnant weather conditions during winter in Northern China may have contributed to the accumulation of VMS. More VMS may have been converted to Si-SOA in this season in wider Northern China and transported to Beijing.

Janecek et al. (2017) estimated the concentrations of D4, D5, and D6 oxidized by OH radicals using the 3-D atmospheric chemical transport model (CMAQ). The inputs of the model included emissions of D4, D5, D6, and their first oxidative species by OH radicals. Meteorological conditions, wet and dry deposition of the primary species were also considered. Reactions of the oxidation products are not included in the model, but the rate constants for the parent cyclic siloxanes reacting with OH radical were applied. The computed concentrations of the oxidation products of D5 (namely o-D5) ranged between 0.37 and 0.81 ng m<sup>-3</sup> when the modeled concentration of D5 ranged between 4.04 and 6.82 ng m<sup>-3</sup> in the USA (Janecek et al., 2017). D5 was the predominant VMS, which accounted for around 60–90% of the sum of L3–L6 and

Table 3  
Si abundance (%) in molecules of major lVMS and cVMS compounds.

Full name	Molecular formula	Molecular weight (g/mol)	Si abundance in molecule (%)	Si abundance in molecule after replacing one H-atom in CH <sub>3</sub> group with one OH group (%)	
L3	Octamethyltrisiloxane	C <sub>8</sub> H <sub>24</sub> O <sub>2</sub> Si <sub>3</sub>	236.53	35.5	33.3
L4	Decamethyltetrasiloxane	C <sub>10</sub> H <sub>30</sub> O <sub>3</sub> Si <sub>4</sub>	310.69	36.0	34.3
L5	Dodecamethylpentasiloxane	C <sub>12</sub> H <sub>36</sub> O <sub>4</sub> Si <sub>5</sub>	384.84	36.4	34.9
L6	Tetradecamethylhexasiloxane	C <sub>14</sub> H <sub>42</sub> O <sub>5</sub> Si <sub>6</sub>	458.99	36.6	35.4
D3	Hexamethylcyclotrisiloxane	C <sub>6</sub> H <sub>18</sub> O <sub>3</sub> Si <sub>3</sub>	222.46	37.8	35.2
D4	Octamethylcyclotetrasiloxane	C <sub>8</sub> H <sub>24</sub> O <sub>4</sub> Si <sub>4</sub>	296.62	37.8	35.8
D5	Decamethylcyclopentasiloxane	C <sub>10</sub> H <sub>30</sub> O <sub>5</sub> Si <sub>5</sub>	370.77	37.8	36.2
D6	Dodecamethylcyclohexasiloxane	C <sub>12</sub> H <sub>36</sub> O <sub>6</sub> Si <sub>6</sub>	444.92	37.8	36.4

D3~D6 (Ahrens et al., 2014; Genualdi et al., 2011; Kierkegaard and McLachlan, 2013). The estimated o-D5 should represent the majority of VMS oxidation products. Hence, the concentrations of SOA in our study are higher than that reported by Janecek et al. (2017), which is reasonable as VMS concentrations in China are much higher than those in the USA (Table 1) (Wang et al., 2001; Kierkegaard and McLachlan, 2013). Milani et al. (2021) also investigated the SOA concentration formed from oxidation of VMS. However, they only quantified one specific SOA compound – hydroxynonamethylcyclopentasiloxane (D4TOH), which is an oxidation product of D5 with one CH<sub>3</sub> group in D5 replaced by OH radical, in PM<sub>2.5</sub> samples collected at two urban locations in the United States. The D4TOH concentration in the samples ranged from 16 to 185 pg m<sup>-3</sup> in Atlanta and 19–206 pg m<sup>-3</sup> in Houston.

On 11th and 12th August, the SO–Si (<DL) and its relative abundance in water-soluble Si were much lower than those of the other days. The surface net solar radiation on 11th ( $3.8 \times 10^5 \text{ J m}^{-2}$ ) and 12th ( $2.8 \times 10^5 \text{ J m}^{-2}$ ) were the third lowest and the lowest during summer days, respectively, while the total cloud cover was 0.98 and 0.94, respectively, which were the highest during the summer campaign. Lower surface net solar radiation and higher total cloud cover hinder the formation of Si-SOA. In the following, we further explored the relationship to secondary inorganic ions (sulfate and nitrate), and possible effects of meteorological conditions on the formation of Si-SOA.

### 3.4. Relationship between SO–Si and secondary inorganic ions

The correlation between SO–Si and secondary inorganic ions (sulfate and nitrate) and sulfur conversion ratio was investigated. The sulfur conversion ratio was calculated as the sulfur concentration in sulfate divided by its concentration in the sum of sulfur dioxide and sulfate. As shown in Table 4, PM<sub>2.5</sub> and secondary inorganic ions are all negatively correlated with SO–Si and SO–Si/PM<sub>2.5</sub>, suggesting SO–Si is unlikely to share the same sources and/or formation mechanisms as secondary inorganic ions. Kim and Xu (2016) reported that VMS can be sorbed to atmospheric aerosols by partitioning, and also interact with them like other volatile species through sorption processes on the particle surfaces and the subsequent heterogeneous reactions. Some of aerosols such as carbon black and sea salts reversibly interacted with VMS whereas other aerosols such as sulfates showed highly irreversible sorption for the VMS, especially at low concentrations. It is interesting to note that ammonium sulfate can significantly increase aerosol yield in very low RH conditions (RH <10%) in an environmental chamber, as it can act as seed particle to form Si-SOA (Wu and Johnston, 2017). However, the negative correlations between sulfate with SO–Si ( $r = -0.57$ ), and sulfate with SO–Si/PM<sub>2.5</sub> ( $r = -0.71$ ) suggest that formation mechanisms of Si-SOA is different under the high RH during our study periods (50–60%). A less negatively correlated SO<sub>4</sub><sup>2-</sup> with SO–Si ( $r = -0.36$ ) and SO–Si/PM<sub>2.5</sub> ( $r = -0.36$ ) in winter could be the combined result of more in-situ Si-SOA formation during the accumulation phase in stagnant winter conditions and/or more external inputs from upwind areas (due to a longer lifetime, see Table 2). However, due to limited samples and investigations into the Si-SOA formation mechanisms in this study, more work is needed to clarify these mechanistic issues.

**Table 4**

The correlations (r) between SO–Si and SO–Si/PM<sub>2.5</sub> with sulfate, nitrate and sulfur conversion ratio.

	Summer		Winter	
	SO–Si	SO–Si/PM <sub>2.5</sub>	SO–Si	SO–Si/PM <sub>2.5</sub>
PM <sub>2.5</sub>	-0.51	-0.64	-0.44	-0.46
SO <sub>4</sub> <sup>2-</sup>	-0.57	-0.71	-0.36	-0.36
NO <sub>3</sub> <sup>-</sup>	-0.60	-0.56	-0.42	-0.50
S-SO <sub>4</sub> <sup>2-</sup> /(S-SO <sub>4</sub> <sup>2-</sup> + S-SO <sub>2</sub> )	-0.56	-0.74	-0.33	-0.28

### 3.5. Relationship between SO–Si and meteorological parameters

The Pearson correlation coefficients (r) of SO–Si and SO–Si/PM<sub>2.5</sub> ratio with different meteorological parameters in summer and winter are presented in Table 5.

SO–Si was positively correlated with surface net solar radiation (ssr,  $r = 0.76$ ) and downward UV radiation at the surface (uvb,  $r = 0.75$ ) in summer (Table 5). Its relative abundance in PM<sub>2.5</sub> was also positively correlated with net solar radiation ( $r = 0.57$ ) and downward UV radiation ( $r = 0.54$ ) in summer. These results indicate that higher solar radiation may favour the formation of Si-containing SOAs. Temperature showed no correlation with SO–Si, suggesting that temperature-dependent emissions of VMS are unlikely to be a key factor in influencing SO–Si concentration. Wind speed was also correlated with SO–Si and SO–Si/PM<sub>2.5</sub> in winter. This is in contrary to the negative correlation between wind speed and PM<sub>2.5</sub> concentrations. This may be due to the higher wind speeds facilitating the transport of VMS and SO–Si from surrounding areas to the sampling location in central Beijing. Relatively humidity (RH), total cloud cover (tcc), and total precipitation (tp, summer only) were all negatively correlated with Si-SOA in summer; only RH is correlated (but weakly) with SO–Si and Si-Si/PM<sub>2.5</sub> in winter. These results suggest that high RH and total cloud cover may hinder the Si-SOA formation or accumulation in the air. Precipitation may enhance wet deposition of Si-SOA. Because the major degradation pathway of atmospheric VMS is through oxidation by hydroxyl radical, which produces hydroxylated methyl groups with lower hydrophobicity than the VMS (Xiao et al., 2015), the Si-SOA can be readily removed from the atmosphere by wet deposition (Atkinson, 1991; Xiao et al., 2015). It is not totally clear why high RH may suppress Si-SOA formation. This may be related to the OH radical concentration, but we do not have data to investigate this further. No previous chamber studies have looked at VMS oxidation under high RH conditions.

In Table 5, no strong correlation was observed between SO–Si and meteorological parameters, except wind speed, in winter. This suggests different factors control the abundance of Si-SOA in summer and winter.

### 3.6. Atmospheric implications

Si-SOA contribute to  $0.06 \pm 0.07\%$  and  $0.16 \pm 0.22\%$  of PM<sub>2.5</sub> mass in winter and summer, but it could contribute up to 0.9% during certain days (Fig. 2). The mass concentration of Si-SOA in Beijing is comparable to widely studied isoprene oxidation products such as 2-methyltetrol organosulfate but lower than total isoprene organosulfates (Bryant et al., 2020). The relative contribution to PM<sub>2.5</sub> mass will likely increase in the future as the PM<sub>2.5</sub> in Beijing is decreasing while no regulation is in place for Si-containing VOCs. The relative importance of Si-SOA to PM<sub>2.5</sub> in more remote locations, such as over the open ocean downwind major Si-VOC source regions, may be much higher, considering the

**Table 5**

Correlation coefficient (r) between SO–Si concentration and meteorological data in summer and winter.

	Summer		Winter	
	SO–Si	SO–Si/PM <sub>2.5</sub>	SO–Si	SO–Si/PM <sub>2.5</sub>
Wind speed	0.28	0.26	0.51*	0.49*
Temperature	0.37	0.14	-0.01	0.19
Relative humidity	-0.75**	-0.69**	-0.47*	-0.46*
Surface net solar radiation	0.76**	0.57*	-0.02	-0.20
Downward UV radiation at the surface	0.75**	0.54*	-0.01	-0.11
Total cloud cover	-0.52	-0.39	0.10	0.20
Total precipitation	-0.55*	-0.46	- <sup>a</sup>	-

\* Correlation is significant at the 0.05 level ( $p < 0.05$ ; two-tailed).

\*\* Correlation is significant at the 0.01 level ( $p < 0.01$ ; two-tailed).

<sup>a</sup> There is no precipitation in winter sampling period.

longer lifetime of VMS (days) at more remote locations (i.e., due to lower OH concentrations) (Table 1). Li et al. (2017a) revealed through chemical mapping of individual particles collected during a research cruise over the Yellow Sea that, the sulfate was coated with a layer of Si. Such coatings of Si on sulfate could not possibly be primary silicon which is extremely insoluble. The coating suggests that they must be secondary Si, formed from VMS. Back trajectory analyses indicated that air masses reaching the cruise were mainly from mainland China (Li et al., 2017a). More work is needed to quantify the concentration of Si-SOA in remote atmospheres as well as their relative abundance in PM<sub>2.5</sub>. In addition, as it exists in fine particles and is much more water soluble than the VMS, Si-SOA could potentially cause greater environmental risks. However, current knowledge on the potential toxicity of the Si-SOA compounds is limited. Furthermore, this study also provides a quantitative method for investigating the oxidation efficiency of VMS through the quantification of SO-Si concentrations directly. Such a method can be used to quantify Si-SOA yield under different environmental conditions in chamber studies.

#### 4. Conclusions

This work provided a conservative estimation of SO-Si and Si-SOA for the first time with no requirements for information on the precursor concentrations. The estimated Si-SOA concentrations were  $12.7 \pm 10.2$  and  $36.6 \pm 23.9$  ng m<sup>-3</sup> in summer and winter, respectively, accounting for  $0.06 \pm 0.07\%$  and  $0.16 \pm 0.22\%$  of PM<sub>2.5</sub>. High surface net solar radiation favours the formation of Si-SOA, especially in summer. Gas-phase oxidation is the predominant Si-SOA formation pathway, rather than the formation on particle surfaces, such as those of SO<sub>4</sub><sup>2-</sup>. Long-range transport is potentially an important source of Si-SOA in Beijing, especially during winter.

#### Credit author statement

Jingsha Xu: Experimental and data analysis, Writing- Original draft preparation, Reviewing and Editing. Zongbo Shi: Conceptualization, Methodology, Reviewing and Editing. Roy M. Harrison: Methodology, Reviewing and Editing. Congbo Song: Reviewing and Editing. Siqi Hou: Reviewing and Editing. Lianfang Wei: Sampling, Reviewing and Editing. Pingqing Fu: Reviewing and Editing. Hong Li: Reviewing and Editing. Weijun Li: Reviewing and Editing.

#### Declaration of competing interest

The authors have no conflict of interests.

#### Acknowledgement

This research was funded by the UK Natural Environment Research Council (NERC, NE/R005281/1; NE/N007190/1) and Royal Society (NAF\R1\191220). The authors gratefully acknowledge the NOAA Air Resources Laboratory (ARL) for the provision of the HYSPLIT transport and dispersion model and/or READY website (<https://www.ready.noaa.gov>) used in this publication.

#### Appendix A. Supplementary data

Supplementary data to this article can be found online at <https://doi.org/10.1016/j.chemosphere.2021.132377>.

#### References

Ahrens, L., Harner, T., Shoeib, M., 2014. Temporal variations of cyclic and linear volatile methylsiloxanes in the atmosphere using passive samplers and high-volume Air samplers. *Environ. Sci. Technol.* 48, 9374–9381. <https://doi.org/10.1021/es502081j>.

- Alton, M.W., Browne, E.C., 2020. Atmospheric chemistry of volatile methyl siloxanes: kinetics and products of oxidation by OH radicals and Cl atoms. *Environ. Sci. Technol.* 54, 5992–5999. <https://doi.org/10.1021/acs.est.0c01368>.
- Annenkov, Vadim V., Danilovtseva, E.N., Pal'shin, V.A., Verkhovina, O.G.N., Zelinskiy, S. N., Krishnan, U.M., 2017. Silicic acid condensation under the influence of water-soluble polymers: from biology to new materials. *RSC Adv.* 7, 20995–21027. <https://doi.org/10.1039/C7RA01310H>.
- ASTM, 1990. *Annual Book of ASTM Standards, Water and Environmental Technology, Standard Test Method for Silica in Water, 11.01. Designation D 859-88*, Philadelphia.
- ASTM-International, 2016. *Standard Test Method for Silica in Water D859 - 16*.
- Atkinson, R., 1991. Kinetics of the gas-phase reactions of a series of organosilicon compounds with hydroxyl and nitrate(NO<sub>3</sub>) radicals and ozone at 297 ± 2 K. *Environ. Sci. Technol.* 25, 863–866. <https://doi.org/10.1021/es00017a005>.
- Badjagbo, K., Furtos, A., Alae, M., Moore, S., Sauv e, S., 2009. Direct analysis of volatile methylsiloxanes in gaseous matrices using atmospheric pressure chemical ionization-tandem mass spectrometry. *Anal. Chem.* 81, 7288–7293. <https://doi.org/10.1021/ac901088f>.
- Bryant, D.J., Dixon, W.J., Hopkins, J.R., Dunmore, R.E., Pereira, K.L., Shaw, M., Squires, F.A., Bannan, T.J., Mehra, A., Worrall, S.D., Bacak, A., Coe, H., Percival, C. J., Whalley, L.K., Heard, D.E., Slater, E.J., Ouyang, B., Cui, T., Surratt, J.D., Liu, D., Shi, Z., Harrison, R., Sun, Y., Xu, W., Lewis, A.C., Lee, J.D., Rickard, A.R., Hamilton, J.F., 2020. Strong anthropogenic control of secondary organic aerosol formation from isoprene in Beijing. *Atmos. Chem. Phys.* 20, 7531–7552. <https://doi.org/10.5194/acp-20-7531-2020>.
- Buser, A.M., Kierkegaard, A., Bogdal, C., MacLeod, M., Scheringer, M., Hungerb uhler, K., 2013. Concentrations in ambient air and emissions of cyclic volatile methylsiloxanes in Zurich, Switzerland. *Environ. Sci. Technol.* 47, 7045–7051. <https://doi.org/10.1021/es3046586>.
- Bzdek, B.R., Horan, A.J., Pennington, M.R., Janecek, N.J., Baek, J., Stanier, C.O., Johnston, M.V., 2014. Silicon is a frequent component of atmospheric nanoparticles. *Environ. Sci. Technol.* 48, 11137–11145. <https://doi.org/10.1021/es5026933>.
- Chandramouli, B., Kamens, R.M., 2001. The photochemical formation and gas-particle partitioning of oxidation products of decamethyl cyclopentasiloxane and decamethyl tetrasiloxane in the atmosphere. *Atmos. Environ.* 35, 87–95. [https://doi.org/10.1016/S1352-2310\(00\)00289-2](https://doi.org/10.1016/S1352-2310(00)00289-2).
- Chu, B., Dada, L., Liu, Y., Yao, L., Wang, Y., Du, W., Cai, J., D allenbach, K.R., Chen, X., Simonen, P., Zhou, Y., Deng, C., Fu, Y., Yin, R., Li, H., He, X.-C., Feng, Z., Yan, C., Kangasluoma, J., Bianchi, F., Jiang, J., Kujansuu, J., Kerminen, V.-M., Pet aj a, T., He, H., Kulmala, M., 2021. Particle growth with photochemical age from new particle formation to haze in the winter of Beijing, China. *Sci. Total Environ.* 753, 142207. <https://doi.org/10.1016/j.scitotenv.2020.142207>.
- CRCSI, 2010. *Annual Report of China Polysiloxane Market in 2009*, 5. China Silicon Industry.
- Genualdi, S., Harner, T., Cheng, Y., MacLeod, M., Hansen, K.M., van Egmond, R., Shoeib, M., Lee, S.C., 2011. Global distribution of linear and cyclic volatile methyl siloxanes in air. *Environ. Sci. Technol.* 45, 3349–3354. <https://doi.org/10.1021/es200301j>.
- Giacomelli, M.C., Largiuni, O., Piccardi, G., 1999. Spectrophotometric determination of silicate in rain and aerosols by flow analysis. *Anal. Chim. Acta* 396, 285–292. [https://doi.org/10.1016/S0003-2670\(99\)00421-3](https://doi.org/10.1016/S0003-2670(99)00421-3).
- Hasenkopf, C.A., Veghte, D.P., Schill, G.P., Lodoyamba, S., Freedman, M.A., Tolbert, M. A., 2016. Ice nucleation, shape, and composition of aerosol particles in one of the most polluted cities in the world: Ulaanbaatar, Mongolia. *Atmos. Environ.* 139, 222–229. <https://doi.org/10.1016/j.atmosenv.2016.05.037>.
- Horii, Y., Kannan, K., 2008. Survey of organosilicone compounds, including cyclic and linear siloxanes. In: *Personal-Care and Household Products, Archives of Environmental Contamination and Toxicology*, vol. 55, p. 701. <https://doi.org/10.1007/s00244-008-9172-z>.
- Janecek, N.J., Hansen, K.M., Stanier, C.O., 2017. Comprehensive atmospheric modeling of reactive cyclic siloxanes and their oxidation products. *Atmos. Chem. Phys.* 17, 8357–8370. <https://doi.org/10.5194/acp-17-8357-2017>.
- Janecek, N.J., Marek, R.F., Bryngelson, N., Singh, A., Bullard, R.L., Brune, W.H., Stanier, C.O., 2019. Physical properties of secondary photochemical aerosol from OH oxidation of a cyclic siloxane. *Atmos. Chem. Phys.* 19, 1649–1664. <https://doi.org/10.5194/acp-19-1649-2019>.
- Kierkegaard, A., McLachlan, M.S., 2013. Determination of linear and cyclic volatile methylsiloxanes in air at a regional background site in Sweden. *Atmos. Environ.* 80, 322–329. <https://doi.org/10.1016/j.atmosenv.2013.08.001>.
- Kierkegaard, A., Adolfsson-Erici, M., McLachlan, M.S., 2010. Determination of cyclic volatile methylsiloxanes in biota with a purge and trap method. *Anal. Chem.* 82, 9573–9578. <https://doi.org/10.1021/ac102406a>.
- Kierkegaard, A., van Egmond, R., McLachlan, M.S., 2011. Cyclic volatile methylsiloxane bioaccumulation in flounder and ragworm in the humber estuary. *Environ. Sci. Technol.* 45, 5936–5942. <https://doi.org/10.1021/es200707r>.
- Kierkegaard, A., Bignert, A., McLachlan, M.S., 2013. Cyclic volatile methylsiloxanes in fish from the Baltic Sea. *Chemosphere* 93, 774–778. <https://doi.org/10.1016/j.chemosphere.2012.10.048>.
- Kim, J., Xu, S., 2016. Sorption and desorption kinetics and isotherms of volatile methylsiloxanes with atmospheric aerosols. *Chemosphere* 144, 555–563. <https://doi.org/10.1016/j.chemosphere.2015.09.033>.
- Kim, J., Xu, S., 2017. Quantitative structure-reactivity relationships of hydroxyl radical rate constants for linear and cyclic volatile methylsiloxanes. *Environ. Toxicol. Chem.* 36, 3240–3245. <https://doi.org/10.1002/etc.3914>.
- King, B.M., Janecek, N.J., Bryngelson, N., Adamcakova-Dodd, A., Lersch, T., Bunker, K., Casuccio, G., Thorne, P.S., Stanier, C.O., Fiegel, J., 2020. Lung cell exposure to

- secondary photochemical aerosols generated from OH oxidation of cyclic siloxanes. *Chemosphere* 241, 125126. <https://doi.org/10.1016/j.chemosphere.2019.125126>.
- Krogseth, I.S., Kierkegaard, A., McLachlan, M.S., Breivik, K., Hansen, K.M., Schlabach, M., 2013. Occurrence and seasonality of cyclic volatile methyl siloxanes in arctic air. *Environ. Sci. Technol.* 47, 502–509. <https://doi.org/10.1021/es3040208>.
- Lamaa, L., Ferronato, C., Prakash, S., Fine, L., Jaber, F., Chovelon, J.M., 2014. Photocatalytic oxidation of octamethylcyclotetrasiloxane (D4): towards a better understanding of the impact of volatile methyl siloxanes on photocatalytic systems. *Appl. Catal. B Environ.* 156–157, 438–446. <https://doi.org/10.1016/j.apcatb.2014.03.047>.
- Li, W., Xu, L., Liu, X., Zhang, J., Lin, Y., Yao, X., Gao, H., Zhang, D., Chen, J., Wang, W., Harrison, R.M., Zhang, X., Shao, L., Fu, P., Nenes, A., Shi, Z., 2017a. Air pollution–aerosol interactions produce more bioavailable iron for ocean ecosystems. *Sci Adv* 3, e1601749. <https://doi.org/10.1126/sciadv.1601749>.
- Li, Y., Chang, M., Ding, S., Wang, S., Ni, D., Hu, H., 2017b. Monitoring and source apportionment of trace elements in PM<sub>2.5</sub>: implications for local air quality management. *J. Environ. Manag.* 196, 16–25. <https://doi.org/10.1016/j.jenvman.2017.02.059>.
- Lu, Y., Yuan, T., Yun, S.H., Wang, W., Wu, Q., Kannan, K., 2010. Occurrence of cyclic and linear siloxanes in indoor dust from China, and implications for human exposures. *Environ. Sci. Technol.* 44, 6081–6087. <https://doi.org/10.1021/es101368n>.
- Lu, K.D., Hofzumahaus, A., Holland, F., Bohn, B., Brauers, T., Fuchs, H., Hu, M., Häsel, R., Kita, K., Kondo, Y., Li, X., Lou, S.R., Oebel, A., Shao, M., Zeng, L.M., Wahner, A., Zhu, T., Zhang, Y.H., Rohrer, F., 2013. Missing OH source in a suburban environment near Beijing: observed and modelled OH and HO<sub>2</sub> concentrations in summer 2006. *Atmos. Chem. Phys.* 13, 1057–1080. <https://doi.org/10.5194/acp-13-1057-2013>.
- Lu, D.W., Tan, J.H., Yang, X.Z., Sun, X., Liu, Q., Jiang, G.B., 2019. Unraveling the role of silicon in atmospheric aerosol secondary formation: a new conservative tracer for aerosol chemistry. *Atmos. Chem. Phys.* 19, 2861–2870. <https://doi.org/10.5194/acp-19-2861-2019>.
- Markgraf, S.J., Wells, J.R., 1997. The hydroxyl radical reaction rate constants and atmospheric reaction products of three siloxanes. *Int. J. Chem. Kinet.* 29, 445–451. [https://doi.org/10.1002/\(SICI\)1097-4601\(199706\)29:6<445::AID-KIN6>3.0.CO;2-U](https://doi.org/10.1002/(SICI)1097-4601(199706)29:6<445::AID-KIN6>3.0.CO;2-U), 1997.
- Martin, K.R., 2007. The chemistry of silica and its potential health benefits. *J. Nutr. Health Aging* 11, 94–97.
- Milani, A., Al-Naiema, I.M., Stone, E.A., 2021. Detection of a secondary organic aerosol tracer derived from personal care products. *Atmos. Environ.* 246, 118078. <https://doi.org/10.1016/j.atmosenv.2020.118078>.
- Muirhead, L.D., Wicht, K.D., Stocker, M.K., Perry, J., Kayatin, J.M., 2018. A Simple Model to Estimate the Hydroxyl Radical Concentration and Associated DMSD Production Rates from Volatile Methyl Siloxanes in the ISS Atmosphere.
- Navea, J.G., Young, M.A., Xu, S., Grassian, V.H., Stanier, C.O., 2011. The atmospheric lifetimes and concentrations of cyclic methylsiloxanes octamethylcyclotetrasiloxane (D4) and decamethylcyclopentasiloxane (D5) and the influence of heterogeneous uptake. *Atmos. Environ.* 45, 3181–3191. <https://doi.org/10.1016/j.atmosenv.2011.02.038>.
- Pieri, F., Katsoyiannis, A., Martellini, T., Hughes, D., Jones, K.C., Cincinelli, A., 2013. Occurrence of linear and cyclic volatile methyl siloxanes in indoor air samples (UK and Italy) and their isotopic characterization. *Environ. Int.* 59, 363–371. <https://doi.org/10.1016/j.envint.2013.06.006>.
- Rao, Z., Chen, Z., Liang, H., Huang, L., Huang, D., 2016. Carbonyl compounds over urban Beijing: concentrations on haze and non-haze days and effects on radical chemistry. *Atmos. Environ.* 124, 207–216. <https://doi.org/10.1016/j.atmosenv.2015.06.050>.
- Rolph, G., Stein, A., Stunder, B., 2017. Real-time environmental applications and display sSystem: READY, environ. Modell. Softw. 95, 210–228. <https://doi.org/10.1016/j.envsoft.2017.06.025>.
- Rücker, C., Kümmerer, K., 2015. Environmental chemistry of organosiloxanes. *Chem. Rev.* 115, 466–524. <https://doi.org/10.1021/cr500319v>.
- Shi, Z., Vu, T., Kotthaus, S., Harrison, R.M., Grimmond, S., Yue, S., Zhu, T., Lee, J., Han, Y., Demuzere, M., Dunmore, R.E., Ren, L., Liu, D., Wang, Y., Wild, O., Allan, J., Acton, W.J., Barlow, J., Barratt, B., Beddows, D., Bloss, W.J., Calzolari, G., Carruthers, D., Carslaw, D.C., Chan, Q., Chatzidiakou, L., Chen, Y., Crilley, L., Coe, H., Dai, T., Doherty, R., Duan, F., Fu, P., Ge, B., Ge, M., Guan, D., Hamilton, J.F., He, K., Heal, M., Heard, D., Hewitt, C.N., Hollaway, M., Hu, M., Ji, D., Jiang, X., Jones, R., Kalberer, M., Kelly, F.J., Kramer, L., Langford, B., Lin, C., Lewis, A.C., Li, J., Li, W., Liu, H., Liu, J., Loh, M., Lu, K., Lucarelli, F., Mann, G., McFiggans, G., Miller, M.R., Mills, G., Monk, P., Nemitz, E., O'Connor, F., Ouyang, B., Palmer, P.L., Percival, C., Popoola, O., Reeves, C., Rickard, A.R., Shao, L., Shi, G., Spracklen, D., Stevenson, D., Sun, Y., Sun, Z., Tao, S., Tong, S., Wang, Q., Wang, W., Wang, X., Wang, X., Wang, Z., Wei, L., Whalley, L., Wu, X., Wu, Z., Xie, P., Yang, F., Zhang, Q., Zhang, Y., Zhang, Y., Zheng, M., 2019. Introduction to the special issue “In-depth study of air pollution sources and processes within Beijing and its surrounding region (APHH-Beijing)”. *Atmos. Chem. Phys.* 19, 7519–7546. <https://doi.org/10.5194/acp-19-7519-2019>.
- Slater, E.J., Whalley, L.K., Woodward-Massey, R., Ye, C., Lee, J.D., Squires, F., Hopkins, J.R., Dunmore, R.E., Shaw, M., Hamilton, J.F., Lewis, A.C., Crilley, L.R., Kramer, L., Bloss, W., Vu, T., Sun, Y., Xu, W., Yue, S., Ren, L., Acton, W.J.F., Hewitt, C.N., Wang, X., Fu, P., Heard, D.E., 2020. Elevated levels of OH observed in haze events during wintertime in central Beijing. *Atmos. Chem. Phys.* 20, 14847–14871. <https://doi.org/10.5194/acp-20-14847-2020>.
- Sommerlade, R., Parlar, H., Wrobel, D., Kochs, P., 1993. Product analysis and kinetics of the gas-phase reactions of selected organosilicon compounds with OH radicals using a smog chamber-mass spectrometer system. *Environ. Sci. Technol.* 27, 2435–2440. <https://doi.org/10.1021/es00048a019>.
- Song, Y., Xie, S., Zhang, Y., Zeng, L., Salmon, L.G., Zheng, M., 2006. Source apportionment of PM<sub>2.5</sub> in Beijing using principal component analysis/absolute principal component scores and UNMIX. *Sci. Total Environ.* 372, 278–286. <https://doi.org/10.1016/j.scitotenv.2006.08.041>.
- Stein, A.F., Draxler, R.R., Rolph, G.D., Stunder, B.J.B., Cohen, M.D., Ngan, F., 2015. NOAA’s HYSPLIT atmospheric transport and dispersion modeling system. *Bull. Am. Meteorol. Soc.* 96, 2059–2077. <https://doi.org/10.1175/bams-d-14-00110.1>.
- Tang, X., Misztal, P.K., Nazaroff, W.W., Goldstein, A.H., 2015. Siloxanes are the most abundant volatile organic compound emitted from engineering students in a classroom. *Environ. Sci. Technol. Lett.* 2, 303–307. <https://doi.org/10.1021/acs.estlett.5b00256>.
- Tuazon, E.C., Aschmann, S.M., Atkinson, R., 2000. Atmospheric degradation of volatile methyl-siloxane compounds. *Environ. Sci. Technol.* 34, 1970–1976. <https://doi.org/10.1021/es9910053>.
- Wang, X.M., Lee, S.C., Sheng, G.Y., Chan, L.Y., Fu, J.M., Li, X.D., Min, Y.S., Chan, C.Y., 2001. Cyclic organosilicon compounds in ambient air in guangzhou, Macau and nanhai, pearl river delta. *Appl. Geochem.* 16, 1447–1454. [https://doi.org/10.1016/S0883-2927\(01\)00044-0](https://doi.org/10.1016/S0883-2927(01)00044-0).
- Wang, R., Moody, R.P., Koniecki, D., Zhu, J., 2009a. Low molecular weight cyclic volatile methylsiloxanes in cosmetic products sold in Canada: implication for dermal exposure. *Environ. Int.* 35, 900–904. <https://doi.org/10.1016/j.envint.2009.03.009>.
- Wang, Y.Q., Zhang, X.Y., Draxler, R.R., 2009b. TrajStat: GIS-based software that uses various trajectory statistical analysis methods to identify potential sources from long-term air pollution measurement data. *Environ. Model. Software* 24, 938–939. <https://doi.org/10.1016/j.envsoft.2009.01.004>.
- Wang, D.-G., Norwood, W., Alaea, M., Byer, J.D., Brimble, S., 2013. Review of recent advances in research on the toxicity, detection, occurrence and fate of cyclic volatile methyl siloxanes in the environment. *Chemosphere* 93, 711–725. <https://doi.org/10.1016/j.chemosphere.2012.10.041>.
- Whalley, L.K., Slater, E.J., Woodward-Massey, R., Ye, C., Lee, J.D., Squires, F., Hopkins, J.R., Dunmore, R.E., Shaw, M., Hamilton, J.F., Lewis, A.C., Mehra, A., Worrall, S.D., Bacak, A., Bannan, T.J., Coe, H., Percival, C.J., Ouyang, B., Jones, R.L., Crilley, L.R., Kramer, L.J., Bloss, W.J., Vu, T., Kotthaus, S., Grimmond, S., Sun, Y., Xu, W., Yue, S., Ren, L., Acton, W.J.F., Hewitt, C.N., Wang, X., Fu, P., Heard, D.E., 2021. Evaluating the sensitivity of radical chemistry and ozone formation to ambient VOCs and NO<sub>x</sub> in Beijing. *Atmos. Chem. Phys.* 21, 2125–2147. <https://doi.org/10.5194/acp-21-2125-2021>.
- Whelan, M.J., Estrada, E., van Egmond, R., 2004. A modelling assessment of the atmospheric fate of volatile methyl siloxanes and their reaction products. *Chemosphere* 57, 1427–1437. <https://doi.org/10.1016/j.chemosphere.2004.08.100>.
- Wu, Y., Johnston, M.V., 2016. Molecular characterization of secondary aerosol from oxidation of cyclic methylsiloxanes. *J. Am. Soc. Mass Spectrom.* 27, 402–409. <https://doi.org/10.1021/jasms.8b05225>.
- Wu, Y., Johnston, M.V., 2017. Aerosol formation from OH oxidation of the volatile cyclic methyl siloxane (cVMS) decamethylcyclopentasiloxane. *Environ. Sci. Technol.* 51, 4445–4451. <https://doi.org/10.1021/acs.est.7b00655>.
- Xiao, R., Zammit, I., Wei, Z., Hu, W.-P., MacLeod, M., Spinney, R., 2015. Kinetics and mechanism of the oxidation of cyclic methylsiloxanes by hydroxyl radical in the gas phase: an experimental and theoretical study. *Environ. Sci. Technol.* 49, 13322–13330. <https://doi.org/10.1021/acs.est.5b03744>.
- Xu, S., Wania, F., 2013. Chemical fate, latitudinal distribution and long-range transport of cyclic volatile methylsiloxanes in the global environment: a modeling assessment. *Chemosphere* 93, 835–843. <https://doi.org/10.1016/j.chemosphere.2012.10.056>.
- Xu, L., Shi, Y., Cai, Y., 2013. Occurrence and fate of volatile siloxanes in a municipal wastewater treatment plant of Beijing, China. *Water Res.* 47, 715–724. <https://doi.org/10.1016/j.watres.2012.10.046>.
- Xu, S., Kozerski, G., Mackay, D., 2014. Critical review and interpretation of environmental data for volatile methylsiloxanes: partition properties. *Environ. Sci. Technol.* 48, 11748–11759. <https://doi.org/10.1021/es503465b>.
- Xu, L., Shi, Y., Liu, N., Cai, Y., 2015. Methyl siloxanes in environmental matrices and human plasma/fat from both general industries and residential areas in China. *Sci. Total Environ.* 505, 454–463. <https://doi.org/10.1016/j.scitotenv.2014.10.039>.
- Xu, J., Liu, D., Wu, X., Vu, T.V., Zhang, Y., Fu, P., Sun, Y., Xu, W., Zheng, B., Harrison, R.M., Shi, Z., 2020a. Source apportionment of fine aerosol at an urban site of Beijing using a chemical mass balance model. *Atmos. Chem. Phys. Discuss.* 2020, 1–28. <https://doi.org/10.5194/acp-2020-1020>.
- Xu, J., Song, S., Harrison, R.M., Song, C., Wei, L., Zhang, Q., Sun, Y., Lei, L., Zhang, C., Yao, X., Chen, D., Li, W., Wu, M., Tian, H., Luo, L., Tong, S., Li, W., Wang, J., Shi, G., Huangfu, Y., Tian, Y., Ge, B., Su, S., Peng, C., Chen, Y., Yang, F., Mihajlić-Zelić, A., Đorđević, D., Swift, S.J., Andrews, I., Hamilton, J.F., Sun, Y., Kramawijaya, A., Han, J., Saksakulkrai, S., Baldo, C., Hou, S., Zheng, F., Daellenbach, K.R., Yan, C., Liu, Y., Kulmala, M., Fu, P., Shi, Z., 2020b. An interlaboratory comparison of aerosol inorganic ion measurements by ion chromatography: implications for aerosol pH estimate. *Atmos. Meas. Tech.* 13, 6325–6341. <https://doi.org/10.5194/amt-13-6325-2020>.
- Yucuis, R.A., Stanier, C.O., Hornbuckle, K.C., 2013. Cyclic siloxanes in air, including identification of high levels in Chicago and distinct diurnal variation. *Chemosphere* 92, 905–910. <https://doi.org/10.1016/j.chemosphere.2013.02.051>.
- Zhou, H., He, J., Zhao, B., Zhang, L., Fan, Q., Lü, C., Dudagula Liu, T., Yuan, Y., 2016. The distribution of PM<sub>10</sub> and PM<sub>2.5</sub> carbonaceous aerosol in Baotou, China. *Atmos. Res.* 178–179, 102–113. <https://doi.org/10.1016/j.atmosres.2016.03.019>.